Thermal Stability of HCl-Doped-Polyaniline and TiO_2 Nanoparticles-Based Nanocomposites

Mohd Omaish Ansari, Faiz Mohammad

Department of Applied Chemistry, Faculty of Engineering and Technology, Aligarh Muslim University, Aligarh 202002, India

Received 13 March 2011; accepted 7 August 2011
DOI 10.1002/app.35444
Published online 2 December 2011 in Wiley Online Library (wileyonlinelibrary.com).

ABSTRACT: Electrically conductive HCl doped polyaniline (Pani) : titanium dioxide (TiO_2) nanocomposites thin films were prepared by *in-situ* oxidative polymerization of aniline in the presence of different amounts of TiO_2 nanoparticles. Later film casting was done using N-Methyl-2-pyrrolidone (NMP) as a solvent. The formation of Pani : TiO_2 nanocomposites were characterized by Fourier Transform Infra-Red spectroscopy (FTIR), x-ray diffraction (XRD) and thermogravimetric analysis (TGA). The stability of the nanocomposites in terms of direct-current electrical conductivity retention was studied in air by isothermal and cyclic techniques. The films of Pani : TiO_2 nanocomposites were observed thermally more stable under ambient environmental conditions than pure polyaniline film. The stability was seen to be highly dependent on the content of TiO_2 nanoparticles in the nanocomposite films. Due to their high stability, such type of nanocomposites can find place as a replacement material for pure polyaniline in electrical and electronic devices. © 2011 Wiley Periodicals, Inc. J Appl Polym Sci 124: 4433–4442, 2012

Key words: thin films; nanocomposites; morphology

INTRODUCTION

With the breakthrough discovery of the emergence of electrical conductivity of the metallic range in polyacetylene upon reaction with some oxidizing agent, the research in the field of electrically conducting polymers has leaped to unexpectedly amazing heights.[1]

Out of the large number of conducting polymers explored, polyaniline (Pani) deserves prime importance because it possesses the best combination of properties such as low cost, excellent environmental stability, tailorable, and reversible electrical properties by controlled charge-transfer processes.[2–4] This makes polyaniline a versatile material for potential applications as electrodes in primary and secondary batteries,[5,6] microelectronics,[7] sensors and actuators, etc.[8]

Besides several others, titanium dioxide (TiO_2) nanoparticles are extremely appealing because of their excellent physical and chemical properties as well as extensive perceived applications in diverse areas such as coatings, solar cells, and photocatalysis. Recently, on the basis of conducting polymers and inorganic nanoparticles, the nanocomposites have attracted attention as it seems to be the potential route to improve the performance of materials in devices. Several reports on the synthesis of the nanocomposites of Pani with Fe_3O_4,[9] ZnO,[10] ZrO_2,[11] montmorillonite,[12] Au,[13] and Ag[14] nanoparticles have already been published.

There are several reports on the *in situ* synthesis of Pani : TiO_2 nanocomposites. Li et al.[15] studied the photodegradation of methyl orange under sunlight using Pani : TiO_2 nanocomposite as a photocatalyst. Dey et al.[16] studied the electrical and dielectric properties of Pani : TiO_2 nanocomposites and also found that the nanocomposites possess higher dielectric constant than that of Pani or TiO_2. Similarly, Karim et al.[17] studied the electrical properties and found that the electrical parameters are highly dependent on the weight percentage of TiO_2 nanoparticles in the nanocomposites. Thus, most of the TiO_2-based nanocomposites of Pani reported earlier have been prepared in the form of powders. The work on Pani : TiO_2 films has been rarely reported, which seems to be because of the poor processability of Pani. Recently, it has been observed that Pani can be plasticized in some selected solvents such as *N*-methyl 2-pyrrolidone (NMP), tetra methyl urea, formic acid, etc., which offers new opportunities toward the processability of Pani.[18,19]

Several reports published on use of conducting polymers in chemical sensors have successfully exploited the variation of electrical conductivity as a measure of sensing response. A change in electrical property indicates whether the conducting polymer is showing sensing response or not while the magnitude of the change in electrical conductivity indicates its sensitivity toward the chemical specie under observation. Recently, it has been reported that the thin films of Pani and Pani : TiO_2 nanocomposites exhibit

Correspondence to: F. Mohammad (faizmohammad54@rediffmail.com).

faster response, shorter recovery time, and higher sensitivity when exposed to NH_3 at room temperature.[20,21] Since, electrical conductivity is an important parameter that is used to correlate most of the properties leading to a wide variety of applications of the conducting polymers, it needs to be investigated. To the best of our knowledge, no systematic work has yet been reported on the stability of Pani and Pani : TiO_2 films in terms of electrical conductivity retention during accelerated aging experiments. Thus a full paper on this aspect is the need of the hour.

In this study, the authors report the preparation of conducting Pani and Pani : TiO_2 nanocomposite thin films using NMP as a solvent followed by methanol extraction for the removal of trapped NMP. The films were doped with HCl and the electrical parameters were determined. Pani : TiO_2 nanocomposite films showed different electrical behavior depending upon the amount of TiO_2 nanoparticles than that of Pani. The surface morphology and thermal stability in terms of electrical conductivity retention were also investigated.

EXPERIMENTAL

Materials

Aniline from E-Merck India, was purified by distilling twice before use. Titanium dioxide (TiO_2; $\sim$ 50 nm) from MKNANO Canada, NMP from Qualigens, potassium persulfate from CDH India, HCl from CDH India (AR grade), ammonia from E-Merck India and methanol from CDH India were used as received. The water used in these experiments was double distilled.

Preparation of Pani : TiO_2 and Pani nanocomposite films

The nanocomposites of Pani : TiO_2 was prepared by *in situ* oxidative polymerization of aniline in presence of different weight percentage of TiO_2 nanoparticles using potassium persulfate as oxidizing agent. Different weight ratios of TiO_2 nanoparticles to the aniline were taken and TiO_2 nanoparticles were dispersed in 200 mL of 1*M* HCl under ultrasonic bath for 3 h. A total of 25 mL of stock solution A was added dropwise to the dispersion of TiO_2 and was put under constant stirring for 2 h to enable the proper dispersion of TiO_2 nanoparticles in aniline. A total of 100 mL of stock solution B was added drop by drop in the above dispersion of TiO_2 nanoparticles and aniline to polymerize the aniline. The reaction mixture was kept under continuous stirring for 2 h at ice temperature and then refrigerated overnight. The resultant mixture turned slowly into greenish black slurry, which was filtered, washed thoroughly with double distilled water to remove excess acid and potassium persulfate until filtrate became colorless and neutral followed by washing with methanol to remove the polyaniline oligomers. Thus, prepared nanocomposites containing different contents of TiO_2 nanoparticles were dedoped by treating with 1 L of 1*M* aqueous ammonia solution. The nanocomposites were dried at 60°C for 24 h in an air oven later converted into fine powders and were stored in desiccator for further experiments. Pure Pani was prepared similarly by mixing stock solution A and B in the absence of TiO_2 and rest of the procedure was same as that for the nanocomposite. The yield of Pani was measured to be $\sim$ 42% and that of Pani : TiO_2-5 was reported to be $\sim$ 45%. Thus the samples prepared were labeled as Pani(EB) (pure Pani), Pani : TiO_2-1(EB), Pani : TiO_2-2(EB), Pani : TiO_2-3(EB), Pani : TiO_2-4(EB), and Pani : TiO_2-5(EB) for pure Pani emeraldine base (EB) and EB of nanocomposites containing different contents of TiO_2 as evident from Table I. Films of Pani and Pani : TiO_2 nanocomposites were prepared by solvent casting using NMP as solvent. Before experimentation, Pani and Pani : TiO_2 nanocomposite films were doped in 100 mL of 1*M* HCl solution followed by washing with double distilled water and drying at 60°C for 24 h.

TABLE I
Preparation Details of Pani : TiO_2 Nanocomposites

Sample I.D.	Volume of stock solution A taken (mL)	Volume of stock solution B taken (mL)	Weight of TiO_2 nanoparticles taken in 200 mL of 1*M* HCl (g)
Pani	25	100	0.00
Pani : TiO_2-1	25	100	0.05
Pani : TiO_2-2	25	100	0.15
Pani : TiO_2-3	25	100	0.25
Pani : TiO_2-4	25	100	0.35
Pani : TiO_2-5	25	100	0.50

Stock solution A: 200 g of double distilled aniline in 1000 mL of 1*M* HCl.
Stock solution B: 72.5 g of $K_2S_2O_8$ in 1000 mL of 1*M* HCl.

Characterization

The stability of HCl-doped Pani and Pani : TiO_2 nanocomposite films was studied in terms of DC electrical conductivity retention under isothermal and cyclic conditions. In isothermal stability testing, the films were heated at 50, 70, 90, 110, and 130°C in an air oven, the electrical conductivity measurements were performed at an interval of 10 min in the accelerated aging experiments. In cyclic method, the electrical conductivity was measured in the temperature range 40–150°C and the experiment was repeated for five times at an interval of 90 min. The measurements of DC electrical conductivity (σ) and its temperature dependence were performed using a 4-inline probe

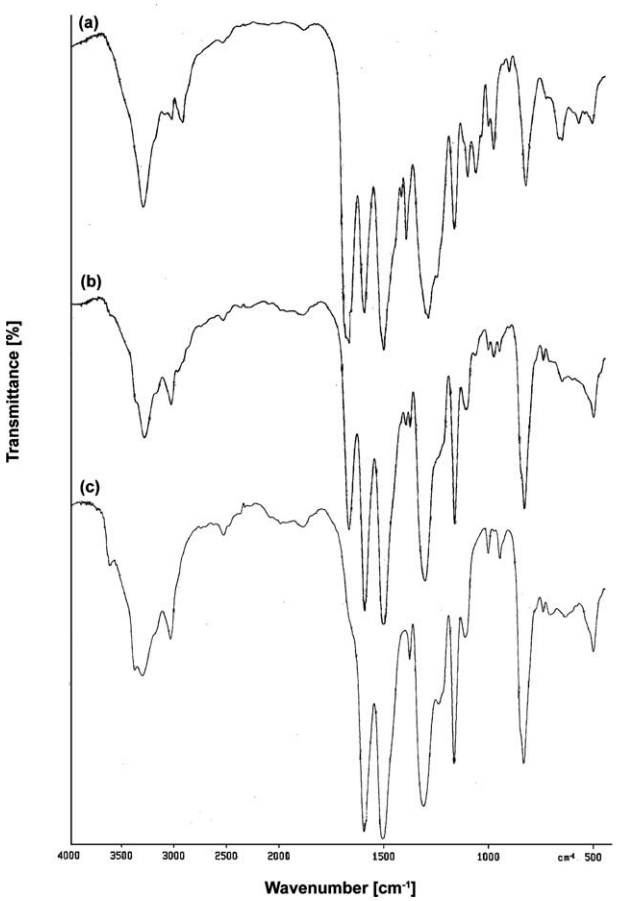

Figure 1 FTIR spectrum of: (a) Pani : TiO_2-0(EB), (b) Pani : TiO_2-5(EB), and (c) Pani : TiO_2-5(EB) after methanol extraction.

electrical conductivity measuring instrument with a temperature controller, PID-200 (Scientific Equipments, Roorkee, India) and calculations was performed using the relation as per the instruction manual of the instrument by the following equation:

$$\sigma = [\ln 2(2S/W)]/[2\pi S(V/I)] \quad (1)$$

where I, V, W, and S are the current (A), voltage (V), thickness of the film (cm), and probe spacing (cm), respectively, and σ is the conductivity (S cm^{-1}).[22]

FTIR spectra were recorded from KBr disks of the nanocomposites. The scanning electron micrograph (SEM) of Pani(EB), Pani : TiO_2-5(EB), and HCl-doped Pani : TiO_2-5 thin films was performed with the help of LEO 435–VF, the samples were gold-coated after that the images were taken. X-ray diffraction (XRD) data were recorded by Bruker D8 diffractometer with Cu Kα radiation at 1.540 Å in the range of $5^\circ \leq 2\theta \leq 70^\circ$ at 40 kV. The thermogravimetric analysis (TGA) was performed on selected samples of the nanocomposites using a Perkin Elmer (Pyris Diamond) instrument in the temperature range from ~ 25 to ~ 800°C at a heating rate of 10°C min^{-1} under nitrogen atmosphere with flow rate of 200 mL min^{-1}.

RESULTS AND DISCUSSION

FTIR spectroscopic studies

The FTIR spectra of Pani(EB) and Pani : TiO_2-5(EB) nanocomposites thin films are shown in Figure 1. The main characteristic peaks of Pani at 3307 and 3034 cm^{-1} can be attributed to the free (non-hydrogen bonded) N–H stretching vibration and intrachain or interchain hydrogen bond between imine sites.[23] The peak at 1595 cm^{-1} is because of C=C stretching mode of the quinoid rings, 1496 cm^{-1} because of C=C stretching mode of benzenoid rings and the peak at about 1291 cm^{-1} can be related to the C–N stretching mode. The peak at 828 cm^{-1} is usually assigned to an out-of-plane bending vibration of C-H of 1,4-disubstituted benzenoid rings, which confirmed the formation of Pani.[24] The characteristic peak of NMP is shifted to a lower value from 1682 cm^{-1} (in case of pure NMP) to 1667 cm^{-1}. The decrease in the intensity of the band corresponding to C=O group of NMP may be attributed to the formation of hydrogen bond between the C=O and imine site of the EB, i.e., C=O...N–H.[18,19,25]

The FTIR spectrum of Pani : TiO_2-5(EB) nanocomposite film is identical to that of Pani(EB) and the relative intensity of the some bands has changed because of the presence of TiO_2 nanoparticles. For example, the bands at 828 and 1421 cm^{-1} have shifted to 834 cm^{-1} and 1401 cm^{-1}, respectively.[16] The characteristic peak of N–H stretching mode at 3307 cm^{-1} of Pani shifted to a lower value at 3297 cm^{-1} in the Pani : TiO_2(EB) nanocomposite. The intensity of band attributed to intrachain or interchain hydrogen bond between imine sites is increased after the incorporation of TiO_2 in the Pani(EB). Thus, it may be inferred from this observation that the incorporation of TiO_2 in the Pani(EB) increases the prevalence of hydrogen bonding in the Pani :

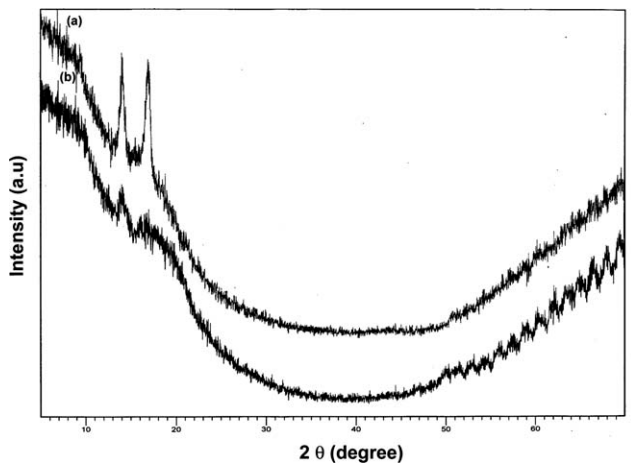

Figure 2 XRD spectrum of: (a) Pani : TiO_2-0(EB) and (b) Pani : TiO_2-5(EB).

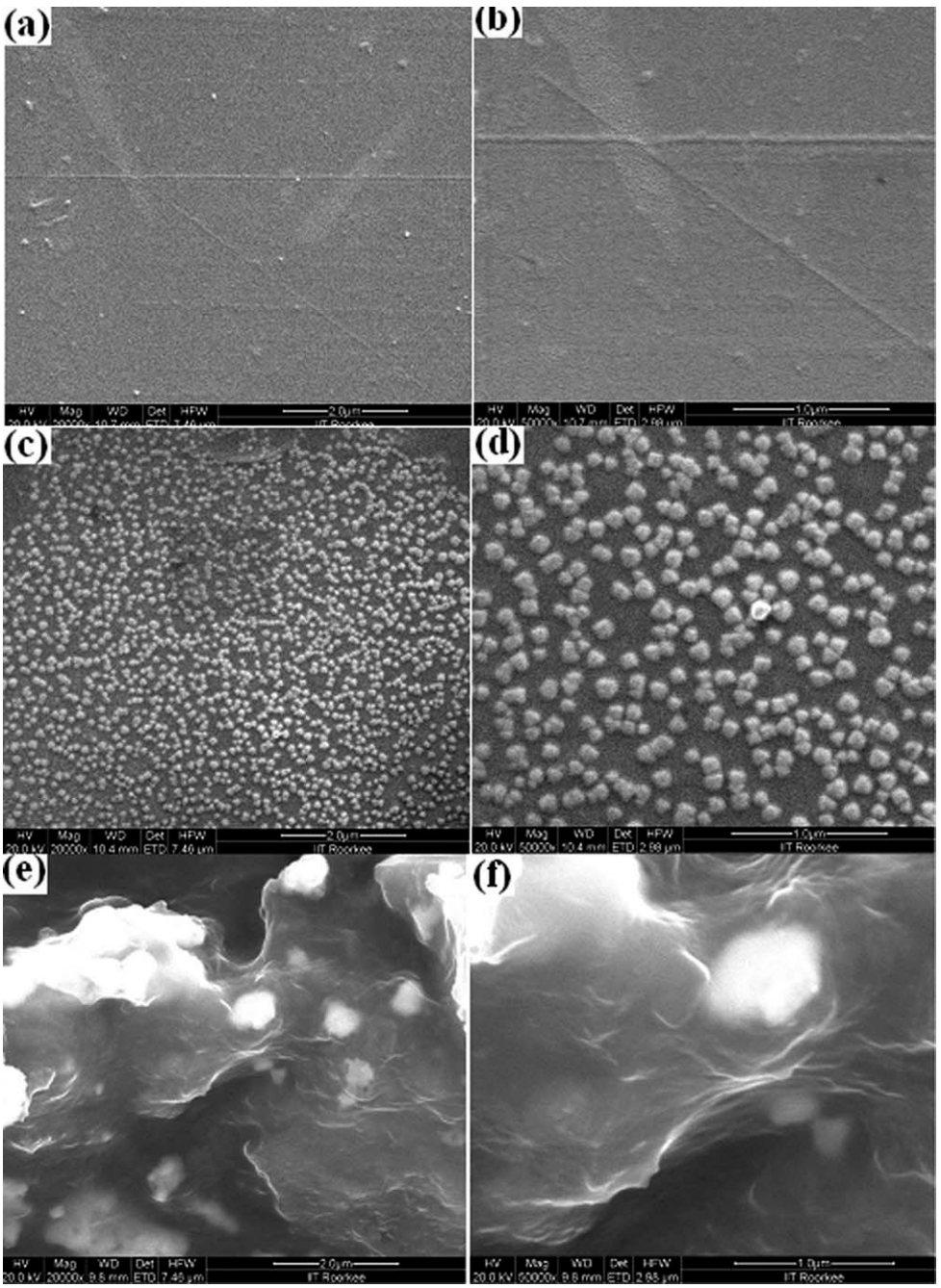

Figure 3 SEM images of: Pani(EB) (a,b), Pani : TiO_2-5(EB) (c,d), and HCl-doped Pani : TiO_2-5 (e, f) films at two magnifications.

TiO_2-5(EB) nanocomposite. The remarkable changes in the FTIR spectrum because of the incorporation of TiO_2 in the Pani(EB) also suggest that there is strong interaction between the Pani and TiO_2 nanoparticles.[26,27]

The characteristic peaks of NMP at 1670 and 1401 cm^{-1} suggest the presence traces of NMP in the nanocomposites, which disappeared completely on extraction with methanol, leading to the decrease in the hydrogen bonding (C=O...N–H) and hence an increase in the intensity of N–H stretching peak at 3307 cm^{-1}.

X-ray diffraction studies

Broad band as seen from Figure 2 in X-ray diffractograms of both Pani(EB) and Pani : TiO_2-5(EB) nanocomposite film indicates highly amorphous nature of both the materials. However, the presence of sharp peaks ($2\theta = 14^\circ$ and 17°) indicates the presence of some crystalline regions in Pani, which may be assigned to the scattering from Pani chains at interplanar spacing. While in the case of Pani : TiO_2-5(EB) nanocomposite film, the peak at $2\theta = 17^\circ$ showed a large decrease in intensity which suggests that the

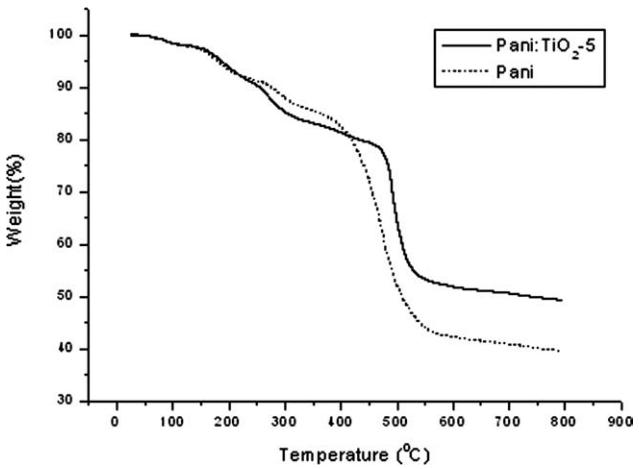

Figure 4 Thermogravimetric analysis of Pani(EB) and Pani : TiO_2-5(EB) nanocomposite films.

addition of TiO_2 nanoparticles increases the amorphous nature of the Pani. The major peak of TiO_2 at $2\theta = 25°$ is not observable while other peaks of TiO_2 in the range of $2\theta = 62–70°$ are very diffuse. It may be pointed out that the Pani(EB) film casted from NMP did not show any crystalline regions and the XRD of film is similar to that of Pani(EB) powder.[28] Similar to this study, Jumali et al.[29] and Lu et al.[30] also reported high amorphous nature of the nanocomposites of Pani : TiO_2 film and PPy : TiO_2 coaxial nanocables, respectively, in their XRD spectra.

Scanning electron micrograph studies

The SEMs of the films of Pani(EB), Pani : TiO_2-5(EB) as well HCl-doped Pani : TiO_2-5 nanocomposites are shown in Figure 3(a–f) at two different magnifications. The uniform morphology without any morphological defects on the surface could be observed in the SEMs of Pani(EB) films as shown in Figure 3(a,b). In case of SEM of Pani : TiO_2-5(EB) film, the TiO_2 nanoparticles are uniformly distributed in the Pani matrix as well as on the surface as evident from the Figure 3(c,d). The surface of HCl-doped Pani : TiO_2 film shows rough morphology and a few clusters of TiO_2 nanoparticles. Similar to this study, Jumali et al.[29] also reported the uniform distribution of spherical TiO_2 nanoparticles in Pani matrix in their nanocomposite films.

Thermogravimetric analysis studies

Thermogravimetric analysis was used to examine the thermal stability of Pani : TiO_2-5(EB) nanocomposites films when compared with Pani(EB). In the case of Pani(EB), it is clear from the Figure 4 that there are three major stages of weight loss, the first weight loss (%) till $\sim$ 120°C is because of the loss of water. The weight loss due to removal of NMP and lower oligomers of Pani occurs in the temperature range from $\sim$ 130 to $\sim$ 400°C. The massive weight loss due to thermo-oxidative decomposition of Pani occurs in the temperature range from $\sim$ 400 to 550°C.[31] Massive weight loss from 400°C onward is due to the thermo-oxidative decomposition of Pani, which may involve the evolution of degradation products such as ammonia, aniline, *p*-phenylenediamine, *N*-phenylaniline, *N*-phenyl-1,4-benzenediamine, carbazole, pyridine-based heterocycle, methane, acetylene, etc.[32] When compared with the TGA of Pani : TiO_2-5(EB) nanocomposites, it may be observed that the degradation of Pani : TiO_2-5(EB) nanocomposite is somewhat similar to that of Pani(EB). The noticeable difference is the high thermal stability of Pani : TiO_2-5(EB) films, the major part of decomposition in the case of Pani(EB) started at 400°C and carried till 550°C and in between total $\sim$ 38% weight loss took place, while in the case of Pani : TiO_2-5(EB) this decomposition temperature is enhanced to 470°C and carried till 540°C, in between $\sim$ 25% weight loss took place. This indicates the increased thermal stability because of the presence of TiO_2 in the nanocomposites, which may involve some stabilizing interaction between Pani and TiO_2.

Electrical conductivity studies

The initial electrical conductivity of HCl-doped Pani film and HCl-doped Pani : TiO_2 nanocomposite

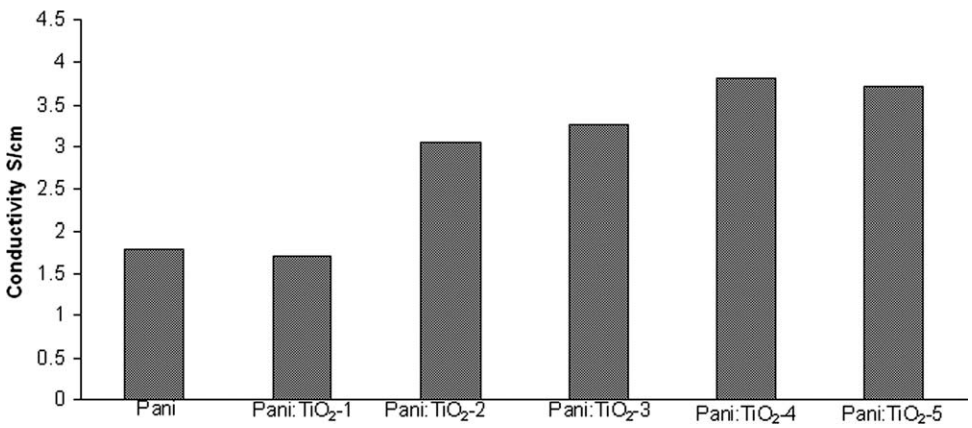

Figure 5 Initial electrical conductivities of HCl-doped nanocomposites films.

TABLE II
Electrical Conductivity Under Isothermal Aging of Pani and Its Nanocomposite Films

Temperature (°C)	Time (min)	Conductivity σ (S cm^{-1}) Pani	Change in relative electrical conductivity/min	Conductivity σ (S cm^{-1}) Pani : TiO_2-1	Change in relative electrical conductivity/min	Conductivity σ (S cm^{-1}) Pani : TiO_2-2	Change in relative electrical conductivity/min	Conductivity σ (S cm^{-1}) Pani : TiO_2-3	Change in relative electrical conductivity/min	Conductivity σ (S cm^{-1}) Pani : TiO_2-4	Change in relative electrical conductivity/min	Conductivity σ (S cm^{-1}) Pani : TiO_2-5	Change in relative electrical conductivity/min
50	0	2.94	0.0096	1.7	0.00898	3.62	0.00498	2.99	0.00008	4.59	0.00245	5.47	0.00385
	10	2.23		1.15		3.41		2.87		4.78		4.96	
	20	2.02		1.14		3.26		2.87		4.19		4.84	
	30	1.9		1.11		3		2.95		4.14		5.08	
	40	1.81		1.09		2.9		2.98		4.14		4.63	
70	0	2.04	0.0092	1.13	0.0062	4.24	0.0095	3.51	0.00377	4.41	0.0063	5.08	0.01185
	10	1.59		0.91		2.85		3.08		3.54		2.93	
	20	1.44		0.87		2.8		3.05		3.43		2.81	
	30	1.35		0.86		2.65		3		3.33		2.7	
	40	1.29		0.85		2.63		2.98		3.3		2.67	
90	0	1.43	0.00945	0.92	0.0068	2.57	0.00935	3.4	0.0067	3.57	0.00847	4.46	0.01457
	10	1.14		0.75		1.95		2.89		2.83		2.31	
	20	1.03		0.72		1.76		2.69		2.59		2.08	
	30	0.94		0.69		1.69		2.59		2.42		1.95	
	40	0.89		0.67		1.61		2.49		2.36		1.86	
110	0	1.01	0.01213	0.74	0.00777	1.71	0.01155	2.79	0.0104	2.57	0.0111	2.02	0.01125
	10	0.73		0.62		1.27		2.15		1.94		1.49	
	20	0.62		0.56		1.08		1.88		1.7		1.34	
	30	0.56		0.53		0.98		1.73		1.54		1.19	
	40	0.52		0.51		0.92		1.63		1.43		1.11	
130	0	0.59	0.0127	0.56	0.00983	1	0.011	1.81	0.01188	1.56	0.01137	1.21	0.01177
	10	0.42		0.44		0.73		1.33		1.17		0.87	
	20	0.35		0.39		0.63		1.09		1.01		0.75	
	30	0.31		0.36		0.59		1.01		0.91		0.68	
	40	0.29		0.34		0.56		0.95		0.85		0.64	

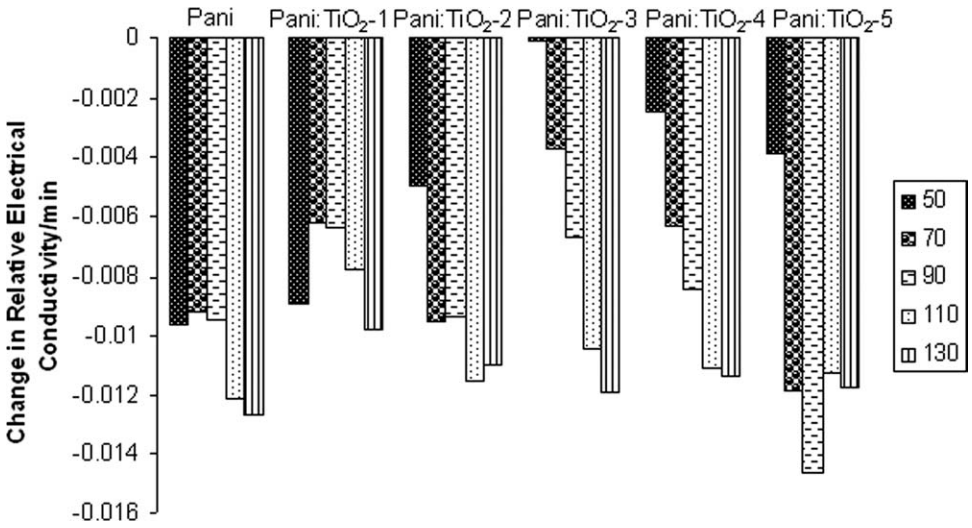

Figure 6 Change in the relative electrical conductivity/minute for HCl-doped nanocomposites films under isothermal aging conditions.

films containing different amount of TiO_2 was measured by 4-inline probe method. From the electrical conductivity measured, it may be concluded that all the samples are semiconducting in nature. It was also observed that the electrical conductivity of the HCl-doped Pani : TiO_2 nanocomposite films solution casted from NMP increases with increase in the TiO_2 nanoparticles content in the nanocomposites as shown in Figure 5. This trend may be attributed to the dominance of the doping effect of TiO_2 in presence of HCl as explained below. However, the trends of continuous decrease[33] or initial increase and then decrease[34] in the electrical conductivity with increase in the TiO_2 nanoparticle content in Pani : TiO_2 nanocomposite powders have been reported. This difference may be attributed to the plasticizing effect of the traces of NMP present in the nanocomposite films in our experiments.

We have prepared Pani(EB) and Pani : TiO_2(EB) nanocomposite films using NMP as a solvent using solvent casting technique. The increase or decrease in electrical conductivity of doped nanocomposite films during different experimentations may be because of various factors competing with each other. The increase in electrical conductivity may be attributed to, for example, (1) the doping by H^+ ions, (2) the annealing effect during heating/aging (isothermal as well as cyclic), (3) the presence of trapped moisture in the nanocomposite films, (4) the plasticizing effect of the traces of solvent (NMP) present, and (5) elevation of temperature because of increase in the number of charge-carriers, etc. The decrease in electrical conductivity may be attributed to, for example, (1) removal of H^+ ions, (2) poor electrical conductivity of the filler (TiO_2), (3) removal of trapped moisture in the nanocomposite films, and (4) degradation of conducting polymer at elevated temperature etc. Another factor that can be considered for increase or decrease in electrical conductivity of the nanocomposite films is the reaction of doping acid, HCl, with TiO_2 nanoparticles. $TiCl_2^{2+}$ may act as doping agent whereas $TiCl_6^{2-}$ may act as dedoping agent as given below[35]:

$$TiO_2 + H^+ + Cl^- \longrightarrow TiO(OH)Cl \quad (2)$$

$$TiO(OH)Cl + 3H^+ + Cl^- \longrightarrow TiCl_2^{2+} + 2H_2O \quad (3)$$

$$TiCl_2^{2+} + 4Cl^- \longrightarrow TiCl_6^{2-} \quad (4)$$

Stability under isothermal aging conditions

The details of electrical conductivity under isothermal aging is presented in Table II. In the case of HCl-doped Pani and Pani : TiO_2 nanocomposite films solution casted from NMP, loss of relative

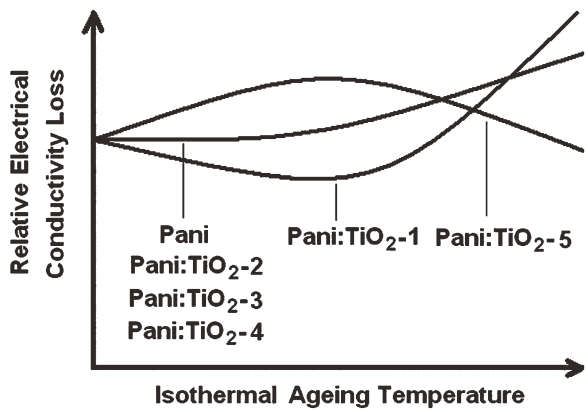

Figure 7 Schematic diagram showing different trends in the variation in the electrical conductivity of nanocomposites films under isothermal aging conditions.

TABLE III
Electrical Conductivity Under Cyclic Aging of Pani and Its Nanocomposite Films

Temperature (°C)	Samples	DC electrical conductivity σ (S cm^{-1}) during				
		Cycle 1	Cycle 2	Cycle 3	Cycle 4	Cycle 5
40	Pani	2.55	0.19	0.13	0.11	0.09
50		2.83	0.22	0.15	0.12	0.10
60		2.64	0.25	0.17	0.14	0.12
70		2.65	0.28	0.19	0.16	0.14
80		2.66	0.32	0.22	0.18	0.16
90		2.69	0.35	0.24	0.20	0.18
100		2.64	0.38	0.27	0.23	0.20
110		2.49	0.43	0.30	0.26	0.23
120		2.40	0.47	0.33	0.28	0.25
130		2.27	0.51	0.37	0.31	0.28
140		1.99	0.56	0.40	0.34	0.31
150		1.57	0.58	0.43	0.37	0.34
40	Pani :	4.77	0.24	0.20	0.11	0.15
50	TiO_2-1	5.50	0.28	0.23	0.13	0.17
60		5.65	0.32	0.26	0.15	0.19
70		5.2	0.34	0.28	0.17	0.21
80		4.27	0.38	0.31	0.19	0.23
90		3.65	0.41	0.33	0.21	0.24
100		3.26	0.45	0.36	0.22	0.25
110		2.89	0.47	0.37	0.23	0.27
120		2.67	0.51	0.39	0.25	0.27
130		2.40	0.53	0.39	0.27	0.28
140		2.09	0.55	0.40	0.29	0.29
150		1.71	0.55	0.39	0.31	0.28
40	Pani :	3.03	0.62	0.63	0.42	0.48
50	TiO_2-2	2.98	0.69	0.69	0.46	0.46
60		3.54	0.75	0.74	0.49	0.547
70		4.00	0.83	0.77	0.53	0.55
80		4.40	0.90	0.81	0.57	0.57
90		5.66	0.97	0.87	0.61	0.59
100		6.92	1.04	0.91	0.65	0.61
110		8.28	1.11	0.95	0.69	0.64
120		9.43	1.20	1.00	0.72	0.65
130		8.49	1.29	1.02	0.75	0.65
140		6.29	1.40	1.05	0.77	0.65
150		4.04	1.52	1.06	0.77	0.649
40	Pani :	3.72	0.81	0.43	0.35	0.34
50	TiO_2-3	3.50	0.92	0.50	0.41	0.39
60		3.65	1.02	0.55	0.46	0.44
70		3.28	1.11	0.63	0.52	0.50
80		4.27	1.21	0.68	0.57	0.56
90		3.65	1.30	0.81	0.64	0.62
100		3.16	1.39	0.83	0.70	0.68
110		2.89	1.48	0.88	0.76	0.74
120		3.12	1.53	0.96	0.82	0.81
130		3.47	1.55	1.02	0.89	0.87
140		3.69	1.56	1.08	0.95	0.91
150		3.78	1.48	1.10	0.98	0.96
40	Pani :	5.56	0.96	0.65	0.53	0.47
50	TiO_2-4	5.95	1.06	0.72	0.60	0.53
60		5.95	1.17	0.79	0.66	0.58
70		5.85	1.29	0.88	0.74	0.63
80		5.56	1.39	0.96	0.80	0.70
90		5.30	1.49	1.04	0.87	0.77
100		4.92	1.60	1.11	0.96	0.82
110		4.53	1.71	1.20	1.02	0.90
120		4.14	1.82	1.28	1.11	0.98
130		3.99	1.93	1.36	1.18	1.04
140		3.65	1.99	1.44	1.25	1.12
150		3.23	2.99	1.48	1.32	1.18

TABLE III. *Continued*

Temperature (°C)	Samples	DC electrical conductivity σ (S cm^{-1}) during				
		Cycle 1	Cycle 2	Cycle 3	Cycle 4	Cycle 5
40	Pani : TiO_2-5	5.50	1.05	0.78	0.63	0.66
50		3.82	1.11	0.86	0.72	0.73
60		4.22	1.24	0.97	0.80	0.80
70		5.57	1.33	1.04	0.86	0.90
80		5.00	1.50	1.14	0.94	0.98
90		3.82	1.61	1.24	1.04	1.11
100		2.06	1.69	1.33	1.12	1.14
110		1.94	1.80	1.42	1.22	1.23
120		1.41	1.92	1.54	1.28	1.32
130		1.04	2.00	1.60	1.37	1.38
140		1.13	2.08	1.69	1.47	1.43
150		1.80	2.11	1.76	1.55	1.46

electrical conductivity is higher at higher temperatures. However, in general, the nanocomposite film containing highest TiO_2 content showed an increase in the relative electrical conductivity loss followed by decrease, whereas the behavior of the nanocomposite film with lowest TiO_2 content is reverse of the former as shown in Figure 6. Although, no regular trend in the relative electrical conductivity loss per minute of heating with increase in temperature of aging was observed, the observations made may be depicted as in the schematic diagram shown in Figure 7 for different formulations. The total loss in relative electrical conductivity during each experiment was divided by the duration of the experiment (40 min) to get the relative electrical conductivity loss per minute of heating as given by the equation:

$$\text{Change in Relative Electrical Conductivity/minute} = \frac{\text{Final Relative Electrical Conductivity at Temperature T} - \text{Initial Relative Electrical Conductivity at Temperature T}}{\text{Duration of experiment (40min)}} \quad (5)$$

The authors have observed from the Figure 6 that the change in relative electrical conductivity per minute increases with increase in temperature of aging and becomes highest at 130°C. It may also be inferred that the presence of TiO_2 in Pani improves the stability of nanocomposites in general.

Stability under cyclic aging conditions

The stability in terms of DC conductivity retention of HCl-doped Pani and Pani : TiO_2 nanocomposite films was also studied by cyclic technique as given in Table III. It may be seen in Figures 8 and 9 that almost all the samples showed an electrical

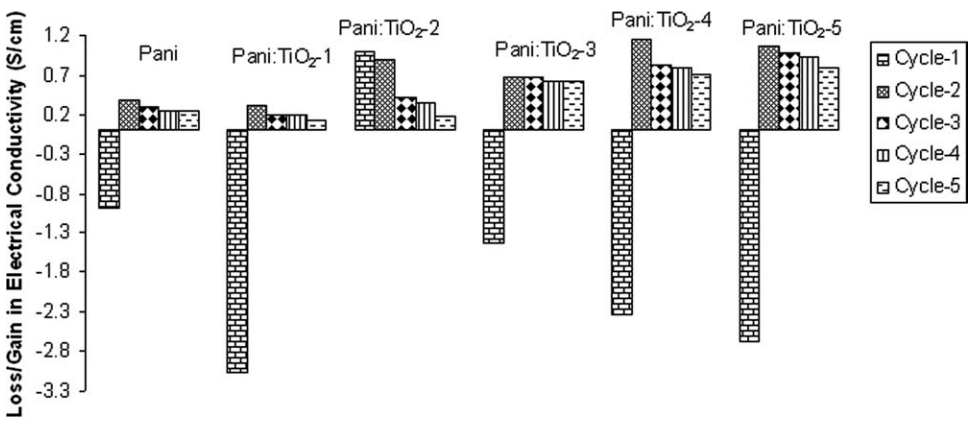

Figure 8 Change in electrical conductivity of HCl-doped nanocomposites films under cyclic aging conditions.

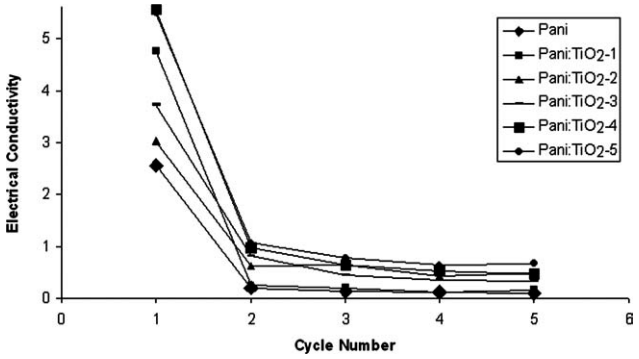

Figure 9 Electrical conductivity at the start of each cycle of HCl-doped nanocomposites films.

conductivity loss in the first cycle. After the first cycle, the electrical conductivity loss is not much different for the next four cycles. It may also be observed from Figure 8 that the change in electrical conductivity between 40 and 150°C increases with increase in the TiO_2 content in the nanocomposites. Similar behavior was also observed for the initial electrical conductivity of the as-prepared nanocomposites, i.e., increase in electrical conductivity with increase in TiO_2 content in the nanocomposites (Fig. 5).

Thus it may be inferred that the nanocomposites are stable semiconductors after first cycle. The difference may be attributed to the removal of moisture, excess HCl or low molecular weight oligomers of aniline. The further difference in the electrical behavior from Cycle 2 onward may be attributed to the continuous annealing effect of temperature cycles. Anomalous behavior of Pani : TiO_2-2 may be attributed to the absence of moisture, excess HCl, and low molecular weight oligomers of aniline in this sample.

CONCLUSIONS

In this study, Pani and Pani : TiO_2 nanocomposite films were synthesized and characterized using different instrumental techniques. We have presented a detailed study of the electrical properties in terms of retention of electrical conductivity under cyclic and isothermal aging conditions. The Pani : TiO_2 nanocomposite films showed greater electrical conductivity and better isothermal and cyclic stability than Pani film. Some anomaly in the electrical property may be because of the removal of surface TiO_2 nanoparticles during doping with HCl. Because of their high stability, such type of nanocomposites can find place as a replacement material for pure Pani in electrical and electronic devices.

Mohd Omaish Ansari is thankful to Dr. S.P. Ansari, Dr. Nazrul Haq, and Mr. Akhtar Ali (Department of Chemistry, Aligarh Muslim University, Aligarh) for their suggestions.

References

1. Shirakawa, H.; Louis, E. J.; MacDiarmid, A. G.; Chiang, C. K.; Heeger, A. J. Chem Commun 1977, 16, 578.
2. Pud, A.; Ogurtsov, N.; Korzhenko, A.; Shapoval, G. Prog Polym Sci 2003, 28, 1701.
3. Zengin, H.; Zhou, W.; Jin, J.; Czrew, R.; Smith, D. W. Jr.; Echegoyen, L.; Carroll, D. L.; Foulger, S. H.; Ballato, J. Adv Mater 2002, 14, 1403.
4. Sainz, R.; Benito, A. M.; Martinez, M. T.; Galindo, J. F.; Sotres, J.; Baro, A. M.; Chauvet, O.; Dalton, A. B.; Baughman, R. H.; Maser, W. K. Nanotechnology 2005, 16, S150.
5. Jang, J.; Bae, J.; Choi, M.; Yoon, S.H. Carbon 2005, 43, 2730.
6. Zhang, J.; Shan, D.; Mu, S. L. J Power Source 2006, 161, 685.
7. He, H.; Zhu, J.; Tao, N. J.; Nagahara, L. A.; Amlani, I.; Tsui, R. J Am Chem Soc 2001, 123, 7730.
8. Tessler, N.; Medvedev, V.; Kazes, M.; Kan, S. H.; Banin, U. Science 2002, 295, 1506.
9. Zhang, Z.; Wan, M. Synth Met 2003, 132, 205.
10. He, Y. Appl Surf Sci 2005, 249, 1.
11. Wang, S.; Tan, Z.; Li, Y.; Sun, L.; Zhang, T. Therm Chim Acta 2006, 441, 191.
12. Shoji, Y.; Ohashi, F.; Ohnishi, Y.; Nonami, T. Synth Met 2004, 145, 265.
13. Yunze, L.; Huang, K.; Yuan, J.; Han, D.; Niu, Li.; Chen, Z.; Gu, C.; Jin, A.; Duvail, J. L. Appl Phys Lett 2006, 88, 162113.
14. Afzal, A. B.; Akhtar, M. J.; Nadeem, M.; Ahmad, M.; Hassan, M. M.; Yasin, T.; Mehmood, M. J. Phys D: Appl Phys 2009, 42, 15411.
15. Li, J.; Zhu, L.; Wu,Y.; Harima, Y.; Zhang, A.; Tang, H. Polymer 2006, 47, 7361.
16. Dey, A.; De, S.; De, A.; De, S. K. Nanotechnology 2004, 15, 1277.
17. Karim, M. R.; Lee, H. W.; Cheong, I. W.; Park, S. M.; Oh, W.; Yeum, J. H. Polym Compos 2010, 31, 83.
18. Zheng, W.; Angelopoulos, M.; Epstein, A. J.; MacDiarmid, A. G. Macromolecules 1997, 30, 2953.
19. Lee, Y. M.; Kim, J. H.; Kang, J. S.; Ha, S. Y. Macromolecules 2000, 33, 7431.
20. Tai, H.; Jiang, Y.; Xie, G.; Yu, J.; Chen, X.; Yu, Z. Sens Actuators B: Chem 2007, 129, 319.
21. Ayad, M. M.; El-Hefnawey, G.; Torad, N. L. J Haz Mat 2009, 168, 85.
22. Al-Ahmed, A.; Mohammad, F.; Rahman, M. Z. A. J Appl Polym Sci 2006, 99, 437.
23. Zhang, L.; Liu, P.; Su, Z. Polym Degrad Stabil 2006, 91, 2213.
24. Wang, P. D.; Chun, Z. H. J Phys Chem C 2009, 113, 8097.
25. Milton, J. A.; Monkman, P. A. J Phys D Appl Phys 1993, 26, 1468.
26. Somani, P. R.; Marimuthu, R.; Mulik, U. P.; Sainkar, S. R.; Amalnerkar, D. P. Synth Met 1999, 106, 45.
27. Niu, Z.W.; Yang, Z. Z.; Hu, Z.B.; Lu, Y. F.; Han, C. C. Adv Funct Mater 2003, 13, 949.
28. Ansari, S. P. D. Phil Thesis, Aligarh Muslim University, 2011,183.
29. Jumali, M. H. H.; Izzuddin, I.; Ramli, N.; Salleh, M. M.; Yahaya, M. Sol Stat Sci Tech 2009, 17, 126.
30. Lu, X.; Zhao, Q.; Liu, X.; Wang, D.; Zhang, W.; Wang, C.; Wei, Y. Macromol Rapid Commun 2006, 27, 43.
31. Chen, S. A.; Lee, H. T. Macromolecules 1993, 26, 3254.
32. Mohammad, F. In Handbook of Organic Conductive Molecules and Polymers; Nalwa, H. S., Ed.; Chichester: John Wiley, 1997; p 834 (and references therein).
33. Xu, J. C.; Liu, W. M.; Li, H. L. Mater Sci and Eng C 2005, 25, 444.
34. Nagaraja, M.; Pattar, J.; Shashank, N.; Manjanna, J.; Kamada, Y.; Rajanna, K.; Mahesh, H. M. Synth Met 2009, 159, 718.
35. Nagesh, K.A. J Phys Chem C 2007, 111, 13028.